

REGOLITH THICKNESS ESTIMATES FROM THE SIZE FREQUENCY DISTRIBUTION OF ROCKY EJECTA CRATERS IN SOUTHWESTERN ELYSIUM PLANITIA, MARS.

N.H. Warner¹, M.P. Golombek², J. Sweeney¹, A. Pivarunas¹. ¹State University of New York at Geneseo, Department of Geological Sciences, 1 College Circle, Geneseo, NY, warner@geneseo.edu, ²Jet Propulsion Laboratory, California Institute of Technology, Pasadena, CA ³U.S. Geological Survey, Flagstaff, AZ.

Introduction: Regolith production by impact gardening is one of the most common geologic processes that operates on rocky planets that lack a dense atmosphere. On Mars, our understanding of regolith production is complicated by a variety of other geologic processes that modify the surface. Along with impact bombardment by bolides that are not winnowed by the thin martian atmosphere, fine-grained components (dust to sand) of the martian regolith are produced through physical (dominantly aeolian) and chemical weathering. Furthermore, volcanic (explosive), fluvial, glacial, and periglacial processes may have contributed significantly to the fine-component sediment supply of Mars while at the same time scouring and removing regolith locally. Because of these complicating factors it is difficult to constrain martian regolith thickness solely using crater production models [1]. Rather, more direct observations and constraints are required that can account for the suite of geologic processes that operated in a region.

Here, we provide an analysis of regolith thickness at southwestern Elysium Planitia using the onset diameter of rocky ejecta craters (RECs) and accounting for local surface processes. The region in our analysis was chosen as the final landing site [2] for the 2016 InSight mission (which will not launch in 2016) and therefore is covered by a uniquely dense set of high resolution images and topography data from the Mars Reconnaissance Orbiter's (MRO) High Resolution Imaging Science Experiment (HiRISE).

Methods: We analyzed regolith thickness over the final 130 km x 27 km InSight landing ellipse (E9) (Fig. 1) using the onset diameter of RECs and crater depth to excavation relationships [3]. All RECs were mapped and their diameters recorded within 17 HiRISE images.

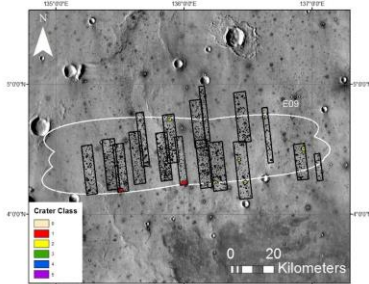


Figure 1: Thermal Emission Imaging System (THEMIS) Daytime IR mosaic with the open, middle, and close orientations of the final landing ellipse for the 2016 InSight (E9). HiRISE images and RECs shown.

Early mapping during the landing site selection process [4] revealed that many small fresh craters lacked rocks in their ejecta. Larger fresh craters on the other hand consistently exhibited rocks (Fig. 2). These observations suggested that smaller impact events may

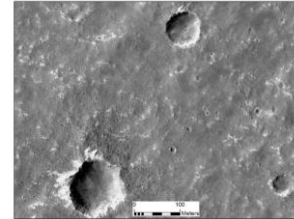


Figure 2: HiRISE image displaying two craters at similar preservation states. The lower 100 m diameter crater in this image exhibits rocks in its ejecta while the other 50 m crater lacks rocks.

have been buffered by a meters-thick regolith while the larger impacts accessed a competent bedrock unit at depth. The maximum depth of excavation of blocks within the continuous ejecta blanket of a simple crater is approximately 0.1 times the transient crater depth, which is 0.084 times the diameter of the final crater [3]. Here, we use the measured diameter of the RECs and assume that the rocky ejecta is derived from a depth of 0.084 times the diameter. We also use the mapped size frequency distribution (SFD) of RECs (excluding non RECs) to quantify the onset diameter bin at which craters stop exhibiting rocks in their ejecta blankets to estimate regolith thickness.

Each REC was classified into 5 classes based on their observed state of modification to help constrain regional rates of crater degradation and thus understand local surface processes (see [5], this meeting). Each crater class was plotted on a cumulative SFD histogram to provide a model age for that class. The estimated degradation rates from these SFDs were used to tease out how crater obliteration might influence our onset diameter estimates if small craters (and the rocks in their ejecta) are preferentially obliterated by subsequent aeolian and impact processes.

Results: Figure 3a displays a cumulative SFD plot for the RECs. Each colored class on this plot represents craters at a different stage of degradation. We classified our craters into 5 total classes, where Class 1 represents the idealized, pristine crater and Class 5 represents the most degraded craterform that still preserves rocks in its ejecta. In this case, Class 2 craters represent the most pristine class considered here because there were not enough Class 1 craters in this region to construct a SFD plot.

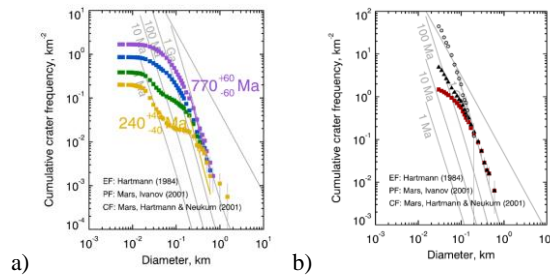


Figure 3a: Cumulative SFD plot showing different preservation classes of the RECs for the 17 HiRISE images. Purple = Class 1 to 5. Blue = Class 1 to 4. Green = Class 1 to 3. Yellow = Class 1 to 2. **3b:** Cumulative SFD plot showing a subset crater count from 3 HiRISE images of only RECs (red squares), all fresh non-RECs (NRECs) + RECs (black triangles), and all craters (open circles).

The oldest SFD (purple) represents all Class 2 to 5 craters. Fitting these data to standard production and chronology functions [6,7] reveals that any crater >200 m in diameter that formed within the last 770 Ma in this region should still preserve rocks in its ejecta blanket. Including only Class 2, the yellow plot indicates that the freshest RECs in this area formed within the last 240 Ma.

Importantly, each plot exhibits a roll-over in the SFD at diameters <200 m suggesting that there are less RECs of this size range than standard crater production models for Mars would predict [6]. We hypothesize that this roll-over could be due to either (1) small crater obliteration or (2) regolith buffering of smaller impact events. In the latter case, a meters-thick regolith could prevent the formation of RECs below a certain threshold size. In the former case, preferential obliteration or resurfacing of smaller craters may have removed them from the population. Using crater morphology and chronology data in Fig. 2 a crater degradation rate of 0.02 m/Myr was calculated for this region [see 5]. Even given that relatively low rate, a 100 m diameter crater (for example) could have been completely obliterated within 500 to 700 Myr, which is close to the maximum age of our most-degraded, yet larger RECs. This suggests that some component of the roll-over in the SFD is related to crater obliteration.

Here we tease out the effect of regolith buffering from crater obliteration so that we can adequately determine an onset diameter for craters with rocks in their ejecta blankets. We do this by mapping all non-rocky but fresh impact craters (NRECs) within a subset region of our data using only 3 HiRISE images. These NRECs share a similar rim and interior crater morphology to the 5 REC classes, yet they lack rocks in their ejecta. We hypothesize that if there is a regolith that buffers an impact event from hitting the competent layer that some percentage of small fresh craters here should lack rocks. By including the fresh NRECs with our 5 REC classes on a SFD plot we evaluated the

magnitude of the roll-over that is solely related to regolith buffering.

Figure 3b provides a cumulative histogram that displays the distribution of all craters ($D > 20$ m) in a subset area (open circles), all 5 classes of RECs (red squares), and all RECs plus fresh NRECs (black triangles). The plot for only the RECs shows a similar roll-over to that seen in Fig. 3a. However, when fresh NRECs are included into this dataset, the slope of the line increases at smaller diameters, approaching an equilibrium slope. The plot of all craters in this region also follows an equilibrium slope.

Discussion and Conclusions: The plots in Fig. 3b can be interpreted as follows: The REC-only plot shows the influence of both regolith buffering and preferential obliteration of small diameter craters. However, the slope of the REC+NREC plot is bolstered by including NRECs. If the original REC roll-over was solely the result of regolith buffering, the inclusion of all fresh rocky and fresh non-rocky craters should follow a production function. If the roll-over was solely the result of obliteration and there was no regolith, then there would be no non-rocky fresh craters to count in the first place. The increase in the slope of the REC+NREC plot suggests that there is a regolith buffering effect. However, the slope still does not follow a production function indicating that crater obliteration is removing some small rock and non-rocky craters here. The slope of the REC+NREC line follows the equilibrium slope for Mars closely, suggesting that the smaller population of craters is likely at equilibrium with degradational processes.

The roll-over of the REC and the REC+NREC curves diverge between 100 and 200 m diameter, suggesting that regolith may be 8.4 to 17 m thick in some places (using [3]). However, the roll-over flat-lines on the REC cumulative plot near the 30 m bin suggesting that the regolith is at least 2.5 m to 3.4 m thick almost everywhere. By subtracting the craters/km² for REC-only data from the REC+NREC data at the 30 m diameter bin we calculated that ~90% of the Insight landing region is covered by a regolith that is at least ~2 to 3 m thick. A similar calculation for the 60 m bin suggests that the regolith is 5 to 6 m thick over ~50% of the area.

References: [1] Hartmann, W.K. et al. (2001). *Icarus* 149. [2] Golombek, M. et. al. (2013). *44th LPSC*, #1691. [3] Melosh, J. (1996), in *Impact Cratering: a Geologic Process*, Oxford Univ. Press. [4] Warner, N.H. et al. (2014). *45th LPSC*, #2217. [5] Sweeney et al. (2016). *47th LPSC*, this meeting. [6] Ivanov, B.A. (2001). *Space Sci. Rev.*, 96. [7] Hartmann, W.K. and Neukum, G. (2001). *Space Sci. Rev.*, 96.